NUMERICAL STUDY OF ELECTRON RELAXATION IN DOPED QUANTUM WELLS

P. Sotirelis and K. Hess

Beckman Institute and Coordinated Science Laboratory
University of Illinois at Urbana-Champaign
Urbana, Illinois 61801

Abstract

The intersubband relaxation time of an electron is calculated considering electron-electron scattering and electron-phonon (bulk LO-phonon) scattering in GaAs quantum wells. The relaxation time is derived and numerically evaluated within the random-phase approximation including full multi-subband and frequency dependent screening. The electron scattering due to the coupled system of electrons and phonons is compared with the decoupled scattering where both electron-electron scattering and unscreened electron-phonon scattering are considered separately. It is shown that the intersubband relaxation time is heavily influenced by the electron density in the well.

Introduction

The intersubband relaxation time of an electron in a quantum well has been the subject of recent investigations both experimentally [1] and theoretically [2]. The goal of much of this research has been to determine the two-dimensional nature of the LO-phonons and how it influences the relaxation time. There have been few studies that have focused on how the electron density in the quantum well affects scattering between subbands [3][4]. High electron densities have been linked to rapid thermalization of the electron distribution in quantum wells, indicating a general increase in scattering with electron density [5]. The main goal of our research is to determine the electron density dependence of the intersubband relaxation time.

The intersubband relaxation time is calculated for an electron interacting with a given thermal distribution of electrons and/or the lattice in a single GaAs quantum well. One of the best methods for determining the intersubband relaxation time involves the evaluation of the imaginary part of the electron self-energy in the random phase approximation (RPA) [6]. This method allows the inclusion of the relevant scattering mechanisms – electron-electron and electron-phonon (LO-phonons) – in a prescribed and consistent way which is complicated by the fact that they mutually interact and affect each other [6][7][8]. This is in contrast to considering electron-electron scattering and unscreened electron-phonon scattering separately (and then summing the two contributions).

Due to the complicated form of the equations that describe the electronic screening in the RPA for a multi-subband quantum well [9][10], various approximations such as static screening, the long wavelength limit, the electric quantum limit, or the plasmon-pole approximation are commonplace. These approximations overly simplify or neglect either the single pair or the plasmon excitations which are expected to be important for inelastic scattering. We *numerically* solve the screening equations in the RPA without making any of the above approximations. Also, the overlap of the wavefunctions is included in a form factor that is evaluated algebraically.

A number of simplifying assumptions are made concerning the quantum well structure which is a single GaAs layer between two $Al_xGa_{1-x}As$ regions. The wavefunctions and energies of the electrons are calculated in the effective-mass approximation. Infinite barriers are assumed and band-bending is ignored. The low-frequency dielectric function of the undoped GaAs layer is approximated by that of the bulk lattice (a single oscillator model in which the longitudinal and transverse optical frequencies are considered dispersionless [11]).

Intersubband Relaxation Rate

We evaluate the intersubband relaxation rate from the imaginary part of the electron self-energy in the random phase approximation (RPA) [12]. The off-diagonal elements of the imaginary part of the self-energy are small and therefore neglected [13]. The corresponding intersubband relaxation rate at zero temperature is given by

$$\tau^{-1}_{\mathbf{k}\,i\to j} = \frac{2\pi}{\hbar}\frac{2}{(2\pi)^2}\int d^2q \frac{1}{2\pi}\mathrm{Im}\left[-V^{eff}_{jiij}(\mathbf{q},\omega)\right]\left[\Theta(E_{i\mathbf{k}}-\mu-\hbar\omega)-\Theta(-\hbar\omega)\right] \tag{1}$$

where $V^{eff}_{mnkl}(\mathbf{q},\omega)$ is the matrix element of the effective interaction potential, $\hbar\omega = E_{i\mathbf{k}} - E_{j\mathbf{k}-\mathbf{q}}$ and $\Theta(x)$ is the unit step function. The matrix element $V^{eff}_{mnkl}(\mathbf{q},\omega)$ is determined numerically from the linear system of equations involving the frequency and wave-vector dependent RPA dielectric function and the matrix element of the bare coulomb potential. The RPA dielectric function accounts for the screening of the conduction band electrons. This includes intrasubband and intersubband excitations of both plasmon and single pair varieties [14]. In addition to the dielectric properties of the electrons, the dielectric properties of the lattice can also be included within the framework of the RPA [6] [7] [8].

Results

As an example we evaluate the intersubband relaxation rate for transitions from subband 3 to subband 2 for a quantum well width of 220 Å. The subband energies are then $E_1 = 0.0116$ eV, $E_2 = 0.0464$ eV, and $E_3 = 0.1044$ eV (the renormalization of the subband energy through the interaction is neglected).

The intersubband relaxation rate is plotted versus electron density in Fig. 1a for three different initial electron energies. It is shown that at low densities the relaxation rate increases with electron density. At higher densities the relaxation rate reaches a maximum and then eventually decreases. Note sharp decreases in the rates at certain densities. The rates associated with larger energies have peaks at higher densities. In Fig. 1b the rates are plotted versus the initial electron energy for four different densities (the zero density rate is equivalent to unscreened electron-phonon scattering). At high enough densities the rates can be much larger than at low densities (except at very low energy).

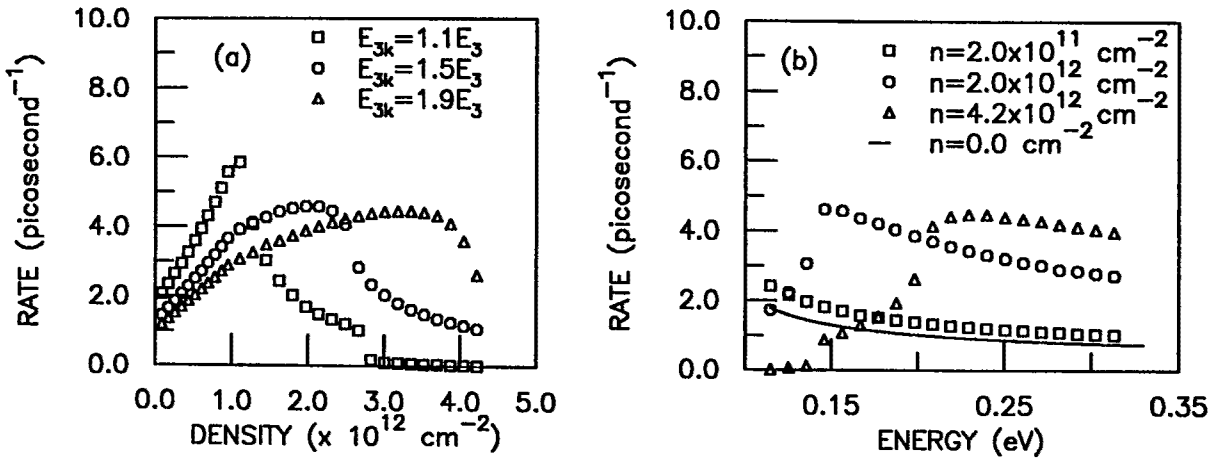

FIG. 1. Electron intersubband relaxation rate due to its interaction with the coupled electron-phonon system for transitions from subband 3 to subband 2 versus electron density (a) and versus electron energy (b). The temperature is zero and the well width is 220 Å.

The above features can be explained by examining the excitations of the coupled electron-phonon system. The coupled plasmon/phonon dispersion and the pair excitation regions are determined from the poles and non-zero regions of $\mathrm{Im}[V^{eff}_{3223}(\mathbf{q},\omega)]$, respectively. The region of integration is determined from energy conservation. Figures. 2a and 2b identify the first sharp rise for the $n = 4.2 \times 10^{12}$ cm^{-2} rate of Fig. 1b as the onset of plasmon emission associated with the $2 \leftrightarrow 1$ excitation. Figures 2c and 2d identify the second and stronger rise in the $n = 4.2 \times 10^{12}$ cm^{-2} rate of Fig. 1b as the onset of plasmon emission associated with the $3 \leftrightarrow 2$ excitation. Figures 2e and 2f identifies the sharp rise in the $n = 2.0 \times 10^{12}$ cm^{-2} rate of Fig. 1b as the onset of plasmon emission associated with the $3 \leftrightarrow 2$ excitation. Note that the $3 \leftrightarrow 2$ intersubband plasmon energy increases with electron density. Because the quantum well is symmetric the other excitations ($1 \leftrightarrow 1$ and $3 \leftrightarrow 1$) do not contribute to the scattering and therefore are absent.

The reduction in the intersubband relaxation rate at high electron densities is investigated in more detail in Fig. 3a. The low energy rate is plotted versus electron density with and without the occupancy of the final states being taken into account. It is shown that the reduction in the rate at high densities is not entirely due to the decrease in the occupancy of final states. Since the $3 \leftrightarrow 2$ intersubband plasmon energy increases with increasing electron density, plasmon emission becomes energetically impossible and the sudden decrease in the rate therefore results. In Fig. 3b the low energy rate is plotted versus electron density and directly compared with the sum of the rate due to electron-electron scattering and unscreened electron-phonon scattering. At low densities the coupled and uncoupled rates agree very well. At higher electron densities the rates due to scattering from the uncoupled electron-phonon system are consistently higher than the coupled electron-phonon system.

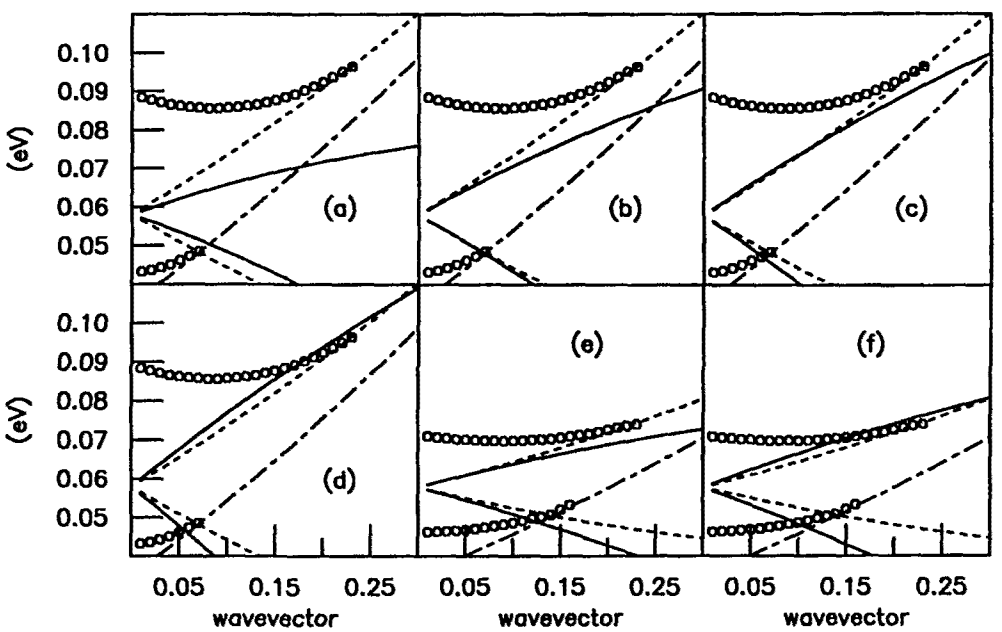

FIG. 2. Plasmon dispersion, single pair excitation regions, and the regions of integration (a), (b), (c), and (d) for electron density $n = 4.2 \times 10^{12}$ cm^{-2}, and (e) and (f) for the electron density $n = 2.0 \times 10^{12}$ cm^{-2}. The electron energies in (a), (b), (c), (d), (e), and (f) are $E_{3k} = 0.125$ eV, $E_{3k} = 0.155$ eV, $E_{3k} = 0.180$ eV, $E_{3k} = 0.210$ eV, $E_{3k} = 0.125$ eV, and $E_{3k} = 0.145$ eV, respectively. The wavevector is normalized to the Fermi wavevector of subband one ((a), (b), (c), and (d), $k_f = 0.4039 \times 10^7$ and (e) and (f) $k_f = 0.3029 \times 10^7$). Circles represent the $3 \rightarrow 2$ and $2 \rightarrow 1$ intersubband plasmon dispersion. The dotted and dashed-dotted lines represent the low wavevector boundaries of the $3 \rightarrow 2$ and $2 \rightarrow 1$ single pair excitation region, respectively. The solid lines represent the low wavevector boundaries of the regions of integration.

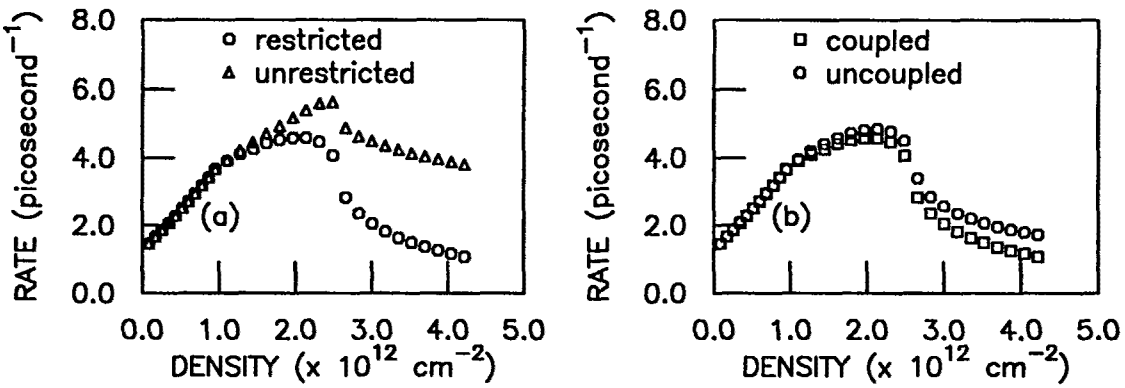

FIG. 3. Electron intersubband relaxation rate due to electron-electron scattering for transitions from subband 3 to subband 2 versus electron density at energy $E_{3k} = 1.5E_3$, with and without the final states restricted by Fermi-Dirac statistics (a) and for the coupled and uncoupled electron-phonon system (b). The temperature is zero and the well width is 220 Å.

Conclusion

The intersubband relaxation rate due to an electron scattering from the coupled electron-phonon system depends significantly on electron density. At high electron densities and energies the rate is much greater than at low electron densities, where the rate depends on energy only weakly. The reduction of the intersubband relaxation rate at high densities is in part due to the restricted availability of final states and in part due to the increase of the $3 \leftrightarrow 2$ intersubband plasmon energy with density. Plasmon emission plays a dominant role in the dependence of the intersubband relaxation rate on electron density and energy. At low densities the coupled and uncoupled rates agree very well, indicating that it is a good approximation to treat electron-electron scattering and electron-phonon scattering as independent scattering mechanisms. At high densities the coupled rates are consistently lower than the uncoupled rates especially at low energy, indicating the screening increases with electron density.

Acknowledgments

We thank Paul von Allmen for valuable discussions. We acknowledge support from National Center for Computational Electronics and the U.S. Office of Naval Research.

References

1 M. C. Tatham, J. F. Ryan, and C. T. Foxon, Phys. Rev. Lett. **63**, 1637 (1989).
2 H. Rücker, E. Molinari, and P. Lugli, Phys. Rev. B 44, 3463 (1991); K. W. Kim and M. A. Stroscio, J. Appl. Phys. **68**, 6289 (1990).
3 S. M. Goodnick and P. Lugli, Phys. Rev. B **37**, 2578 (1988).
4 J. A. White and J. C. Inkson, Phys. Rev. B **43**, 4323 (1991).
5 W. H. Knox et al, Phys. Rev. Lett. **61**, 1290 (1988).
6 G. D. Mahan, *Many-Particle Physics*, (Plenum Press, New York, 1981).
7 L. Wendler and R. Peshtedt, Phys. Stat. Sol. **138**, 197 (1986).
8 R. Jalabert and S. Das Sarma, Phys. Rev. B **40**, 9723 (1989).
9 Eric D. Siggia and P. C. Kwok, Phys. Rev. B **2**, 1024 (1970).
10 J. Lee and H. Spector, J. Appl. Phys. **54**, 6989 (1983).
11 J. S. Blakemore, J. Appl. Phys. **53**, R123 (1982).
12 J. J. Quinn and R. Ferrel, Phys. Rev. **112**, 812 (1958).
13 The ratio of the magnitude of the off-diagonal elements to the diagonal elements were provided by a private communication with Paul von Allmen.
14 J. K. Jain and S. Das Sarma, Phys. Rev. B **36**, 5949 (1987).